# Fabrication of 200 nm period nanomagnet arrays using interference lithography and a negative resist

Maya Farhoud,[a] Juan Ferrera, Anthony J. Lochtefeld, T. E. Murphy,
Mark L. Schattenburg, J. Carter, C. A. Ross, and Henry I. Smith
*Massachusetts Institute of Technology, Cambridge, Massachusetts 02139*

(Received 2 June 1999; accepted 17 August 1999)

Magnetic information storage density has increased at the rate of 60% per year for the past seven years. There is wide agreement that continuation of this trend beyond the physical limits of the continuous thin-film media currently used will likely require a transition to discrete, lithographically defined magnetic pillars. Interference lithography (IL) appears to be the most cost-effective means of producing two-dimensional arrays of such pillars. IL can rapidly expose large areas with relatively simple equipment, without the need for a mask, and with fine control of the ratio of pillar diameter to period. We show that negative-tone imaging yields three times the contrast of positive-tone imaging for the generation of holes in photoresist, suitable for subsequent deposition or electroplating of magnetic material. We use a negative *i*-line, chemically-amplified resist (OHKA THMR-iN PS1) to form 200 nm period arrays of magnetic dots in Co and Ni. Such arrays, with a variety of well controlled diameters, are used to study the effect of particle size on magnetic behavior. © *1999 American Vacuum Society.* [S0734-211X(99)06806-7]

## I. INTRODUCTION

Lithographically defined, discrete, magnetic nanoparticles (or ''nanomagnets'') have been the subject of research over the past several years.[1–4] The interest in nanomagnets stems from the fact that they would enable data densities to be extended beyond what is possible with continuous magnetic data storage media. In a recording scheme based on nanomagnets, each discrete particle will be magnetized in one of two possible polarities to indicate a binary one or zero.[5] In order to study the feasibility of magnetic data storage in discrete nanoparticles, as well as to design the optimal nanomagnet for a storage application, many groups have found interference lithography (IL) to be the lithography of choice.[3,4,6] IL offers advantages over scanning electron-beam lithography due to its ability to define grid patterns over large areas in a single, fast, maskless exposure. In addition, since IL defines periodic patterns with well-controlled periodicity, it provides an absolute reference that may facilitate read/write head position tracking.

Previously, we employed our IL system (Fig. 1) to generate a 200 nm period array of holes in a positive resist and electrodeposited magnetic nickel and cobalt pillars.[4] We found the pillars to be strongly interacting, and thus unsuitable for data storage. In order to achieve improved control of the dimensions of holes patterned by IL, and, therefore, the spacing between neighboring magnetic pillars, a negative tone process is preferred.[7] Negative tone imaging with a 351 nm wavelength interference lithography scheme has been demonstrated using image reversal to achieve 320 nm period arrays.[8] In this work, we report a demonstration of IL in a negative, chemically amplified photoresist (OHKA THMR-iN PS1). We have successfully patterned 200 nm period gratings as well as arrays of holes with precisely controlled diameters down to 56 nm. Using this imaging process, we fabricated and characterized arrays of magnetic dots with a fixed pitch and a variety of diameters. Our ability to control the geometry of the magnetic particles is critical to the study of lithographically patterned magnetic recording media.

## II. WHY NEGATIVE-TONE IMAGING?

In interference lithography, the image is formed by exposing resist to a standing wave formed by the interference of two coherent waves of equal amplitude. This generates a pattern of lines in the resist with a period equal to $\lambda/2\sin\theta$, where $\lambda$ is the wavelength of the light, and $\theta$ is half the angle between the two beams (Fig. 1). Two-dimensional (2D) grid patterns are readily generated by rotating the substrate 90° after the first exposure, and performing a second exposure. Assuming equal exposure times for the two exposures, the incident dose distribution is the superposition of two perpendicular sinusoidal standing waves, which can be expressed as

$$I=A\sin^2\left(\frac{\pi}{p}X\right)+A\sin^2\left(\frac{\pi}{p}Y\right), \tag{1}$$

where $A$ is the peak dose in each standing wave, and $p$ is the period of the interference pattern. A plot of Eq. (1) is shown in Fig. 2(a). The peaks correspond to the superposition of the maxima of the perpendicular $X$ and $Y$ sinusoids, the minima correspond to the superposition of two minima, and the saddle points separate consecutive maxima and minima. The dose at the peaks is $2A$, at the minima is 0 assuming the incident beams are exactly matched, and at the saddle point is $A$. When imaging 2D structures, such as arrays of holes or arrays of posts in photoresist, one can choose to define these features either at the minima or the maxima, depending on the polarity of the resist used. We illustrate in Figs. 2(b) and 2(c) that a higher contrast, and hence, a broader process lati-

[a]Electronic mail: maya@nano.mit.edu

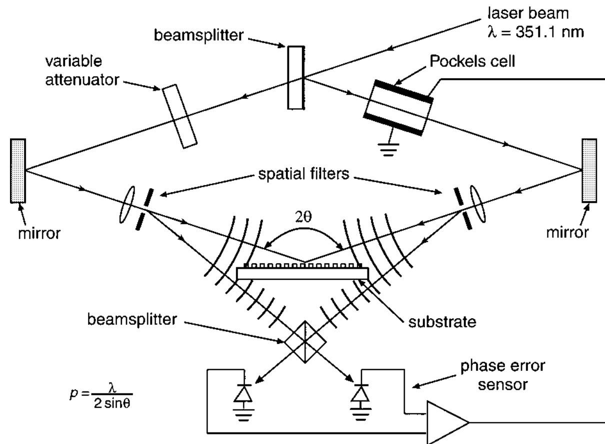


FIG. 1. Schematic of the interference lithography system (Ref. 9). A 351 nm argon ion laser is split into two arms which are spatially filtered by a lens and pinhole. The two arms recombine at the resist coated substrate where their interference pattern is recorded.

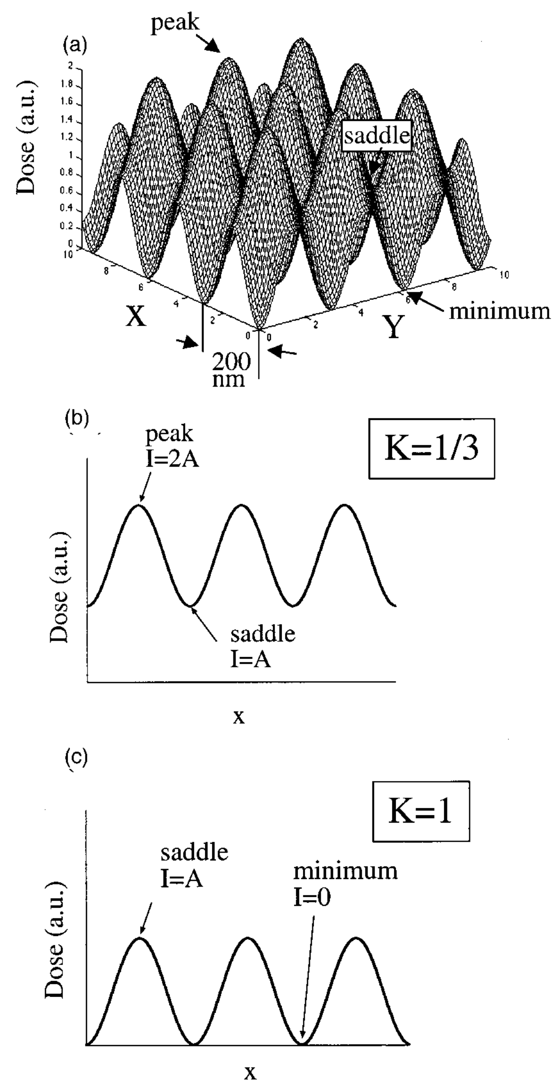


FIG. 2. (a) Plot of total dose distribution impinging upon the resist as a result of the superposition of two perpendicular grating exposures of equal amplitude. The dose at the peaks is twice the dose at the saddle points. At the minima the dose is zero. (b) Cross section through the peaks and saddle points. In this case, the contrast $K=(I_{\max}-I_{\min})/(I_{\max}+I_{\min})=1/3$. (c) Cross section through the saddle points and minima. The contrast is $K=1$.

tude is realized if the critical features (the holes or the posts) are imaged at the minima. That is, the minima can be used to expose posts in positive resists or holes in negative resists. If one were, for example, to use the maxima in Fig. 2(a) to expose holes in a positive resist, then areas in between the holes would receive a dose (i.e., $A$) equal to half that at the hole locations (i.e., $2A$). This would have the consequence of reduced image contrast and greatly reduced exposure latitude. Image contrast, which is defined as $K=(I_{\max}-I_{\min})/(I_{\max}+I_{\min})$ is equal to 1/3 in Fig. 2(b), which represents a cut through the maxima, and is equal to unity in Fig. 2(c), which represents a cut through the minima. Hence, with IL, it is preferable to use positive resists to create posts and negative resists to create holes.

The issue of whether to use a positive or a negative resist in IL also arises in the fabrication of gratings in which the linewidth is not equal to the space width. To treat this quantitatively, we define the duty cycle of a grating as the ratio of the linewidth to the spatial period, $L/p$. We assume an infinite contrast for the resist, i.e., above a given threshold dose a positive resist is totally removed and below the threshold dose a negative resist is totally removed. Figure 3 plots the change in duty cycle with respect to a change in the dose, as a function of the grating duty cycle.

## III. CHARACTERIZATION OF THMR-iN PS1 NEGATIVE, *i*-LINE PHOTORESIST

In order to create large-area arrays of nanomagnets with dimensions in the 100 nm range, using either electroplating or lift-off, a negative resist is preferred, as discussed earlier. We investigated the chemically amplified negative photoresist THMR-iN PS1, from OHKA America. Figure 4(a) depicts the multilayer stack. The antireflection coating (ARC) is critical to minimize the backreflection into the resist layer, which would otherwise degrade process latitude. We developed an analytical model to calculate this backreflection, given the real and imaginary indices of refraction of the several layers.[9] We adjust the thickness of the ARC (Brewer Science XHR-i) to achieve minimum backreflection. The resist was softbaked on a hot plate at 90 °C for 90 s, and postbaked at 100 °C for 90 s.

Figure 4(b) illustrates the profiles obtained at a dose of 22 mJ/cm$^2$. Figure 5(a) is a plot of grating linewidth as a function of dose. Defining process latitude as the change in the dose necessary to produce a 10% change in linewidth, we estimate a process latitude of about 30%. Figure 5(b) illustrates the process latitude and precise control of hole diameter we achieve with the THMR-iN PS1 negative resist. The process latitude is about 15%.

## IV. NANOMAGNET FABRICATION AND CHARACTERIZATION

The response of the THMR-iN PS1 negative resist, illustrated in Fig. 5(b), enables us to fabricate arrays of magnetic

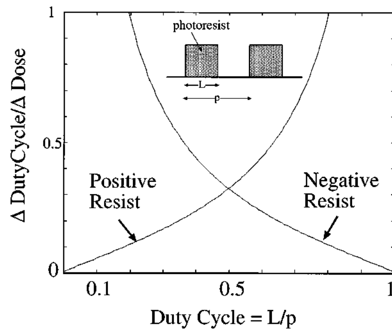


FIG. 3. Comparison, for positive and negative resist, of the change in duty cycle with respect to a change in dose, as a function of the duty cycle. Duty cycle is defined as the ratio of resist linewidth to period. For a duty cycle above 0.5, a negative resist is preferred, i.e., reduced sensitivity of change in duty cycle to change in dose.

dots with a fixed period and a variety of interparticle spacings. We are studying the interactions of ensembles of magnetic dots as a function of the spacing between nearest neighbors. Also, we can study the magnetic behavior of individual dots to determine a correlation to particle geometry (shape and size). Typically, such studies entail determining the particles' easy axis of magnetization and switching fields.

Fabrication of nanomagnets by lift-off is illustrated in Fig. 6. Following exposure by IL of holes in the photoresist, the holes are transferred, via reactive ion etching, into the interlayer oxide and the ARC, using $CHF_3$ and $O_2$, respectively. Either Ni or Co dots are formed by *e*-beam evaporation and lift-off. The oxide and ARC are removed in a 5:1:1 $H_2O$:$H_2O_2$:$NH_4OH$ solution at 80 °C.

We fabricated arrays of Co dots by evaporating 55 and 80 nm of material of into holes in ARC, having a range of diameters between of 120 and 80 nm. The individual Co

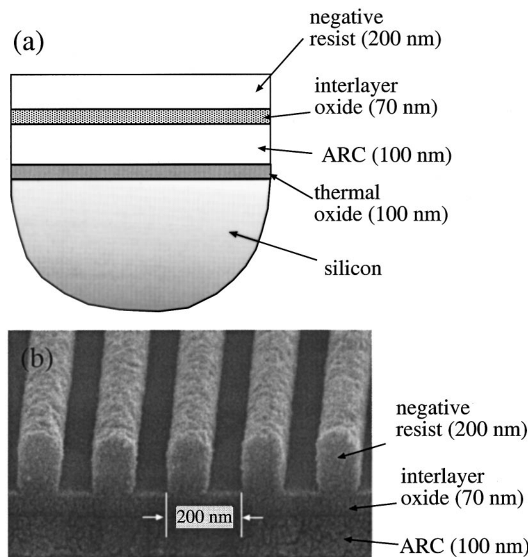


FIG. 4. (a) The trilayer used in interference lithography. Silicon wafers with 100 nm of thermal oxide are coated with ARC, an *e*-beam evaporated oxide and negative photoresist imaging layer. (b) Scanning-electron micrograph of a 200 nm period grating in THMR-iN PS1 negative resist after exposure and development.

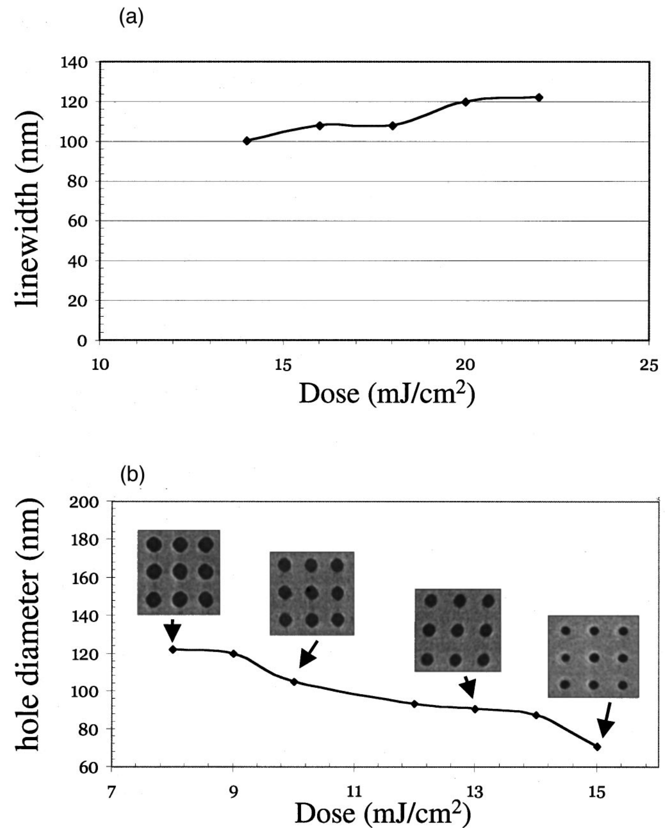


FIG. 5. (a) Plot of grating linewidth exposed in THMR-iN PS1 negative resist, as a function of exposure dose, illustrating process latitude. (b) Plot and micrographs illustrating the dependence of hole diameter on exposure dose in THMR-iN PS1 negative resist.

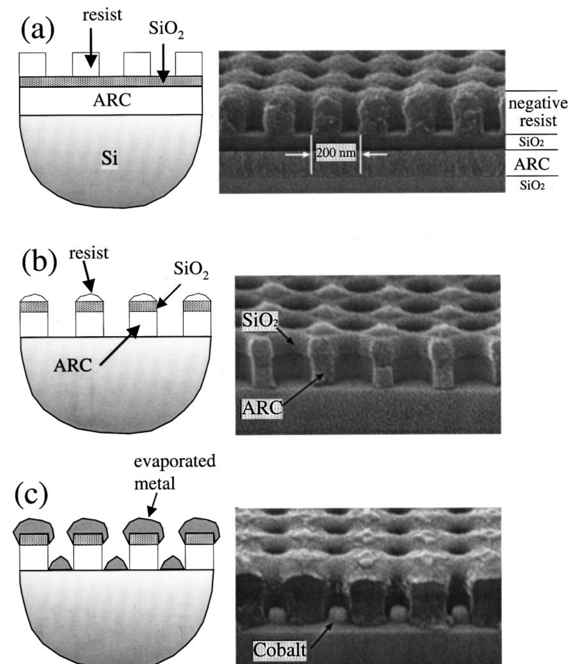


FIG. 6. Graphical depiction and cross-sectional electron micrographs of the three main steps in the fabrication of nanomagnets: (a) holes are exposed in resist with interference lithography, (b) the hole pattern is transferred via reactive ion etching into the interlayer oxide and ARC, and (c) a ferromagnet such as Ni or Co is evaporated via *e*-beam into the oxide ARC template.

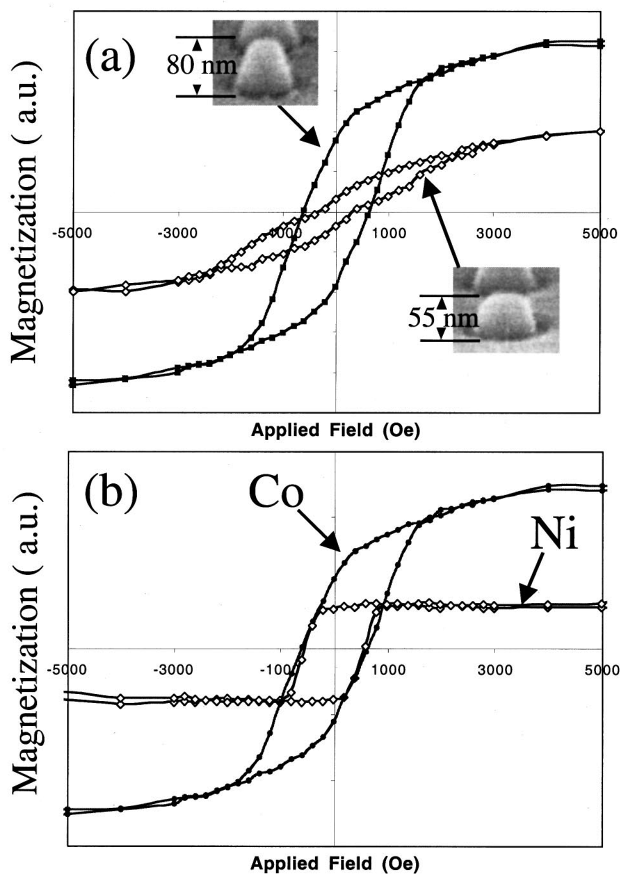


FIG. 7. Magnetization loops obtained by vibrating sample magnetometry for the arrays of 80 nm diameter nanomagnets. (a) Magnetization loops for 55 nm and 80 nm tall Co nanomagnets (scanning-electron micrographs in inset). (b) Magnetization loops for 80 nm tall Co and Ni nanomagnets.

structures are in the shape of truncated cones, as expected for a lift-off process. Magnetic data from a vibrating sample magnetometer indicate that the larger-diameter dots favor in-plane magnetization, while the smaller dots favor out-of-plane magnetization. Also, the squareness, given by the ratio of magnetization at zero applied field to saturation magnetization, is increased by a factor of two for the 80 nm structures [Fig. 7(a)]. We have conducted similar studies using Ni dots instead of Co. Since Ni is a weaker ferromagnet than Co, a smaller magnetic signal is generated. However, Ni nanomagnets with geometries that favor out-of-plane magnetization, generate magnetization loops that are more square than identically sized Co nanomagnets, as illustrated in Fig. 7(b). A squareness of one is desirable in magnetic data storage media.

## V. SUMMARY

To form arrays of nanomagnets suitable for ultrahigh-density data storage, we pattern arrays of holes in a negative resist using interference lithography. For the generation of holes in photoresist, we show that negative-tone imaging yields three times the contrast of positive-tone imaging, and hence, an enhanced process latitude. Negative-tone imaging also enhances the process latitude for patterning gratings in which the lines are wider than the spaces.

We characterized the patterning of gratings and holes with interference lithography in the *i*-line, chemically amplified negative resist, THMR-iN PS1 from OHKA America and successfully produced gratings with a process latitude of 30%, and holes with a process latitude of 25%. The precise control of hole diameters enables the fabrication of nanomagnets with a variety of sizes suitable for studies that correlate magnetic behavior with particle geometry.

## ACKNOWLEDGMENTS

The authors wish to thank James Daley for technical assistance. This work is supported by IBM through an academic fellowship, NSF under Grant No. DMR-9871539 and DARPA.

[1]S. Y. Chou, M. Wei, P. R. Krauss, and P. B. Fisher, J. Vac. Sci. Technol. B **12**, 3695 (1994).
[2]R. L. White, R. M. H. New, and R. F. W. Pease, IEEE Trans. Magn. **33**, 990 (1997).
[3]A. Fernandez, P. J. Bedrossian, S. L. Baker, S. P. Vernon, and D. R. Kania, IEEE Trans. Magn. **32**, 4472 (1996).
[4]M. Farhoud, M. Huang, H. I. Smith, M. L. Schattenburg, J. M. Bae, K. Youcef-Toumi, and C. A. Ross, IEEE Trans. Magn. **34**, 1087 (1998).
[5]S. Y. Chou, Proc. IEEE **85**, 652 (1997).
[6]M. A. M. Haast, J. R. Schuirhuis, L. Abelmann, J. C. Lodder, and Th. J. Pompa, IEEE Trans. Magn. **34**, 1006 (1998).
[7]A. Fernandez, H. T. Nguyeb, J. A. Britten, R. D. Boyd, M. D. Perry, D. R. Kania, and A. M. Hawryluk, J. Vac. Sci. Technol. B **15**, 729 (1997).
[8]J. Y. Decker, A. Fernandez, and D. W. Sweeney, J. Vac. Sci. Technol. B **15**, 1949 (1997).
[9]M. L. Schattenburg, R. J. Aucoin, and R. C. Fleming, J. Vac. Sci. Technol. B **13**, 3007 (1995).